nature metabolism

Supplementary information

https://doi.org/10.1038/s42255-024-01191-9

Short-chain fatty acid metabolites propionate and butyrate are unique epigenetic regulatory elements linking diet, metabolism and gene expression

In the format provided by the authors and unedited

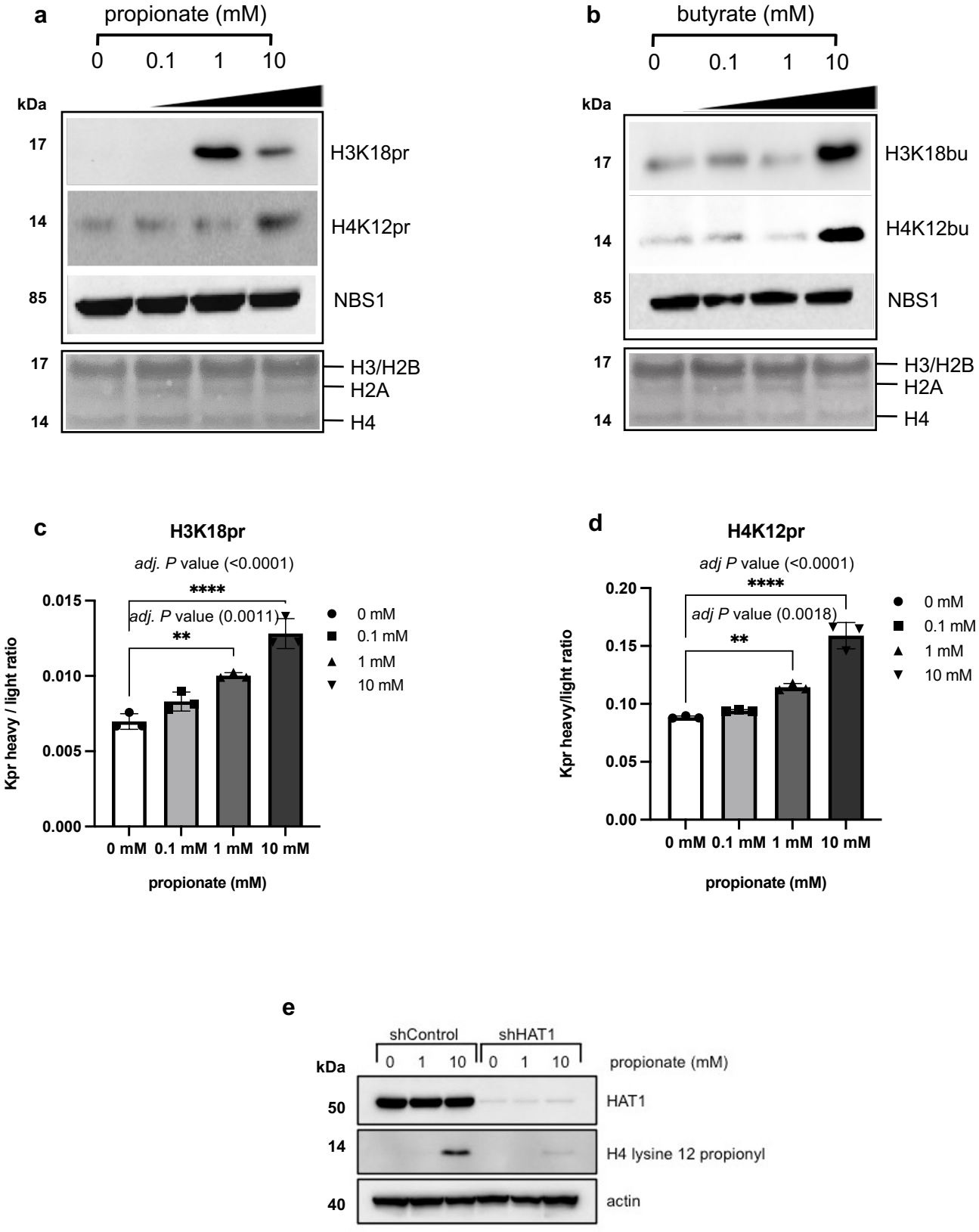

Supplementary Fig. 1 | Immunoblots of acid-extracted **a** H3K18/H4K12pr and **b** H3K18/H4K12bu histone marks at 0 – 10 mM sodium propionate/butyrate treatments with anti-NBS1 as control (top). SDS-PAGE of histones H2A/B, H3/H4 (bottom). Dose-dependent ^{13}C-propionate incorporation into H3 and H4 as measured by increases in the heavy/light propionyl lysine containing peptides. Heavy/light propionyl lysine containing peptides representing **c** H3K18pr and **d** H4K12pr levels at 0, 0.1, 1, and 10 mM ^{13}C-propionate supplementation (mean ± SD, n = 3). Multiple comparisons by ordinary, one-way ANOVA followed by hypothesis testing using the Bonferroni correction method with 0.05 *P* value cutoff. ***P* < 0.01, **** *P* < 0.0001 **e** Depletion of HAT1 diminishes incorporation of propionate into the H4 lysine 12 site.

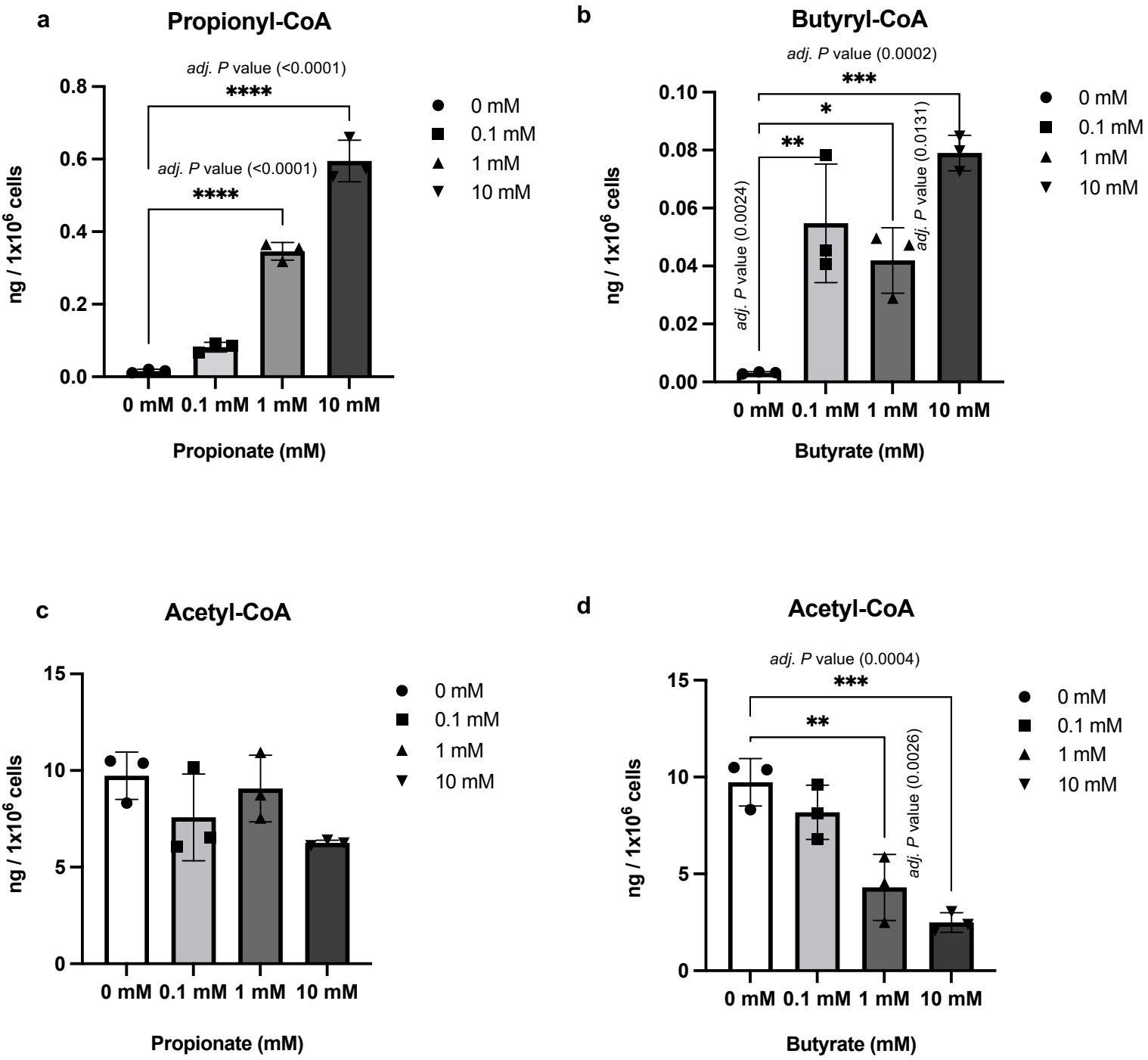

Supplementary Fig. 2 | Quantitative analysis of acyl-CoA levels by LC-MS/MS following SCFA supplementation. **a** Dose-dependent increases in **a** Propionyl-CoA and **b** Butyryl-CoA levels upon increasing propionate and butyrate supplementation at 0, 0.1, 1, and 10 mM. Acetyl-CoA levels upon increasing **c** propionate and **d** butyrate supplementation. Quantitative analysis was done by multiple reaction monitoring (MRM) using an internal standard approach. Calculated Acyl-Co concentrations in each sample were normalized to the number of cells (mean ± SD, n = 3). Multiple comparisons by ordinary, one-way ANOVA using hypothesis testing followed by Bonferroni correction method with 0.05 *P* value cutoff. **P* < 0.05, ***P* < 0.01, ****P* < 0.001, *****P* < 0.0001.

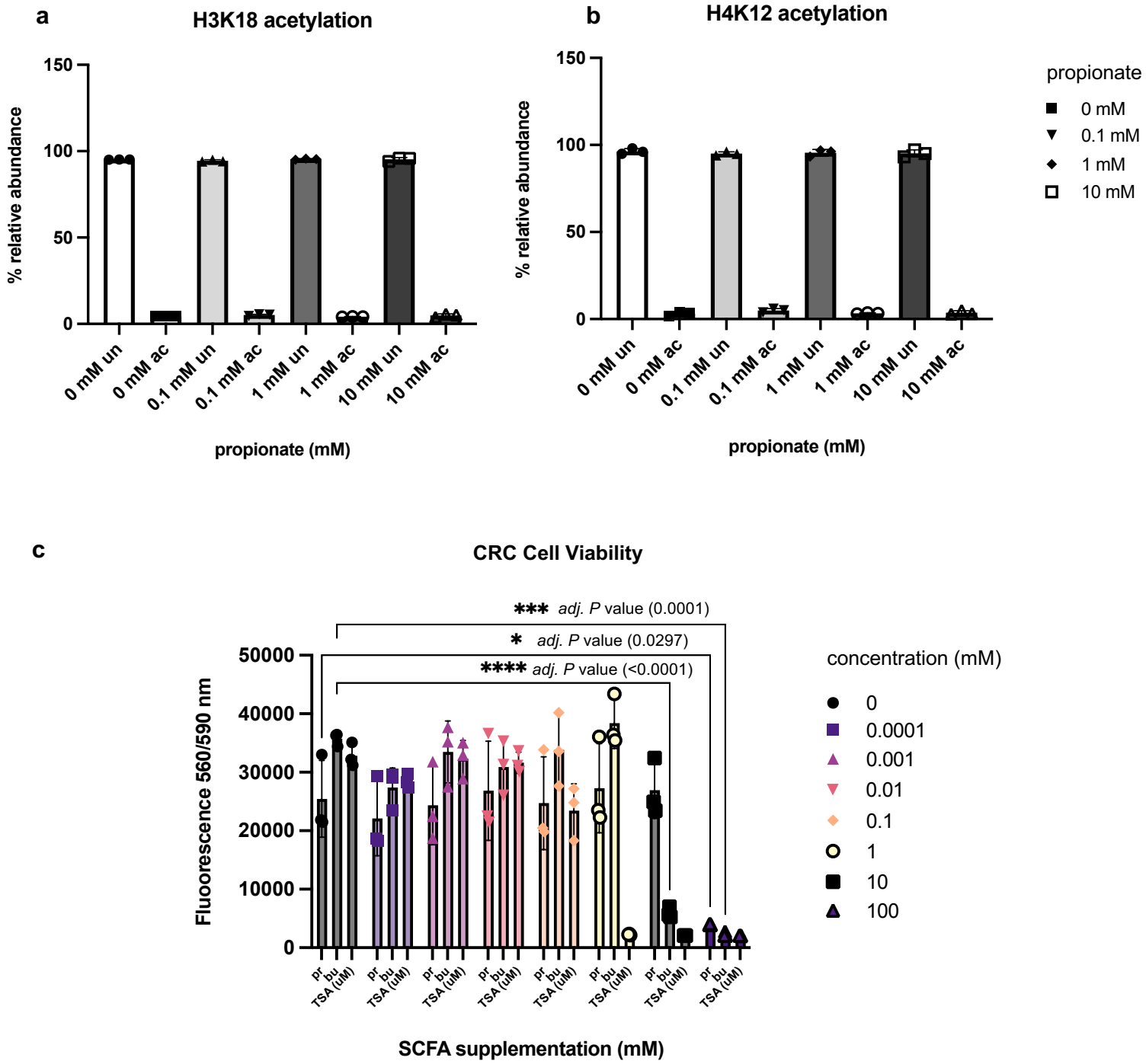

Supplementary Fig. 3 | H3 and H4 acetylated vs unmodified states as a function of propionate supplementation. Relative abundances of acetylated vs unmodified states on **a** H3K18 **b** H4K12 **c** H3K9 and **d** H3K23 following 0, 0.1, 1, and 10 mM propionate supplementation (mean ± SD, n = 3). **e** CRC cell viability as a function of NaPr and NaBu supplementation over 72 hrs. as measured by CellTiter-Blue® fluorescence assay. TSA, a known HDAC inhibitor with IC50 ~ 2 nM was used as a negative control on a μM level. (mean ± SD, n = 3). Multiple comparisons by two-way ANOVA using statistical hypothesis testing followed by Bonferroni correction method with 0.05 *P* value cutoff. *$P < 0.05$, ***$p < 0.001$, ****$p < 0.0001$.

a

Enrichment FDR	nGenes	Pathway Genes	Fold Enrichment	Pathways
7.9E-08	56	86	1.9	Colorectal cancer
6.1E-09	82	135	1.8	Apoptosis
3.6E-10	95	157	1.8	Hippo signaling pathway
1.5E-08	110	200	1.6	Focal adhesion
1.5E-08	111	202	1.6	Proteoglycans in cancer
8.0E-08	115	217	1.6	Reg. of actin cytoskeleton
7.7E-11	174	331	1.6	Human papillomavirus infection
9.3E-08	127	246	1.5	Shigellosis
6.7E-08	148	294	1.5	MAPK signaling pathway
4.7E-13	265	530	1.5	Pathways in cancer

c

H3K18pr CRC targets			Prop RNA-seq	
symbol	fold	FDR	fold	p-adj
CTNNB1	3.00	2.05E-11	-0.61	4.65E-09
TCF20	3.01	9.54E-11	-0.34	0.080547
LEF1	2.72	9.49E-06	-1.26	2.65E-05
CCND1	3.85	4.08E-21	-0.46	1.56E-05
MYC	2.08	9.55E-06	1.93	4.66E-67
FOS	2.99	1.97E-12	1.56	7.67E-36
JUN	2.67	3.03E-06	1.57	8.08E-09

b

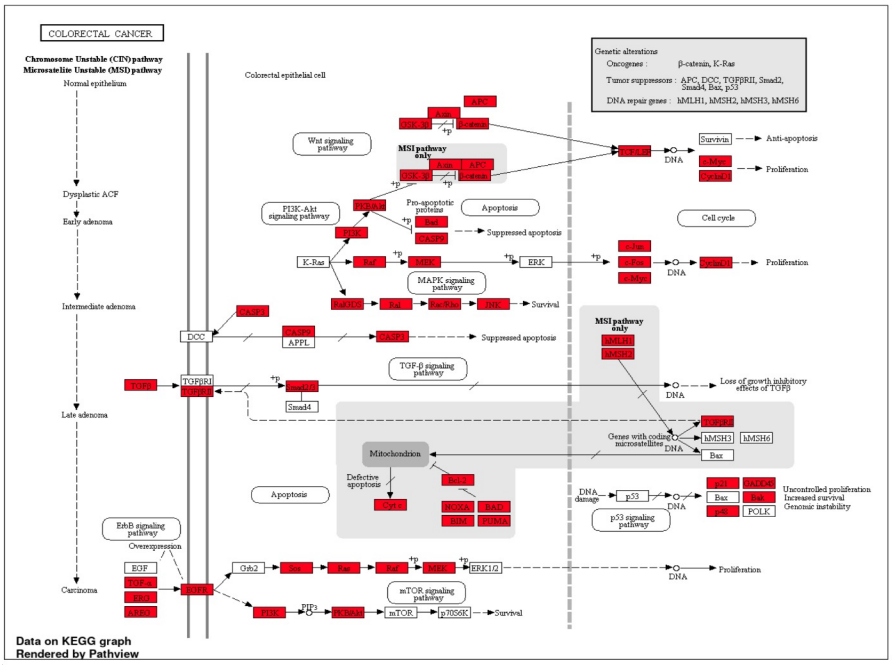

d

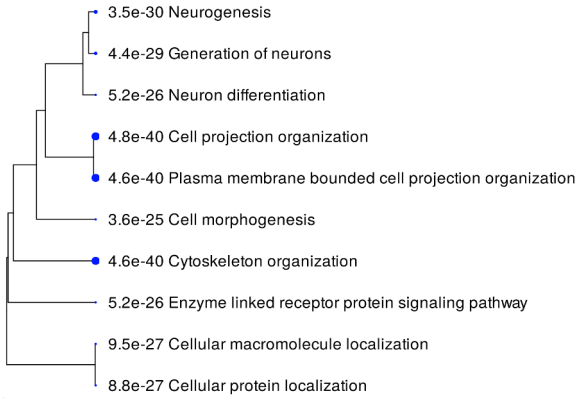

e

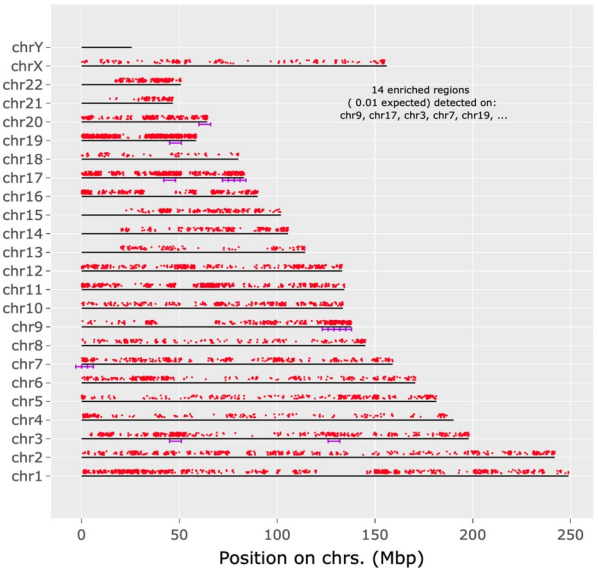

Supplementary Fig. 4 | KEGG pathway analysis of H3K18pr-associated genes. **a** Top ten pathways with their number of genes and log2 fold enrichment. FDR is calculated from a nominal *P* value obtained from a hypergeometric test (FDR < 0.05). Fold enrichment is calculated as percentage of H3K18pr differentially bound genes associated with a pathway divided by the corresponding percentage in input. **b** CRC KEGG pathway enrichment by Pathview. Genes that are overrepresented compared to input are in red. **c** H3K18pr-associated differential binding of key CRC genes and log2 fold changes in their expression levels, as determined by differential RNA-seq of 10 mM treated vs. untreated conditions. n = 3 experimental replicates per condition (FDR < 0.05). **d** Hierarchical clustering tree summary of correlations among significant pathways in H3K18pr-associated annotated genes. Hierarchical clustering of the pathways was performed using ShinyGO. Pathways were clustered together based on shared genes and gene enrichment analysis was performed using two-sided Fisher's exact test, and FDR correction was applied to adjust for multiple comparisons in the pathway analysis and hierarchical clustering. Size of dots indicates statistically significant FDR adjusted (FDR < 0.05) *P* values. **e** Chromosomal position of H3K18pr-associated regions represented by red dots. Purple lines represent statistically significant enrichment compared to input. The genome was scanned with a sliding window (size 6 Mb) further subdivided into 2 equal-sized steps for sliding. Within each window a hypergeometric test was used to test for enrichment over input. FDR-adjusted *P* value cutoff for window was 1E-05. Chromosomes may be partly shown due to scaling to last genes location. Gene chromosomal mapping was performed using ShinyGO.

a

Enrichment FDR	nGenes	Pathway Genes	Fold Enrichment	Pathways
4.6E-11	104	134	1.6	Ribosome
4.5E-10	116	157	1.6	Hippo signaling pathway
2.0E-08	103	142	1.5	Spinocerebellar ataxia
9.4E-09	120	169	1.5	Protein processing in endoplasmic reticulum
4.5E-10	203	306	1.4	Huntington disease
2.0E-08	167	252	1.4	Endocytosis
2.3E-11	240	363	1.4	Amyotrophic lateral sclerosis
1.9E-12	307	475	1.4	Pathways of neurodegeneration
3.4E-09	243	383	1.3	Alzheimer disease
7.6E-09	838	1527	1.2	Metabolic pathways

c

H4K12pr CRC targets			Prop RNA-seq	
symbol	fold	FDR	fold	p-adj
CTNNB1	3.17	5.90E-15	-0.61	4.65E-09
TCF20	3.26	0.000136	-0.34	0.080547
LEF1	2.01	0.0019	-1.26	2.65E-05
CCND1	2.8	5.54E-14	-0.46	1.56E-05
MYC	2.4	2.09E-11	1.93	4.66E-67
FOS	3.05	1.28E-07	1.56	7.67E-36
JUN	3.32	7.54E-18	1.57	8.08E-09

b

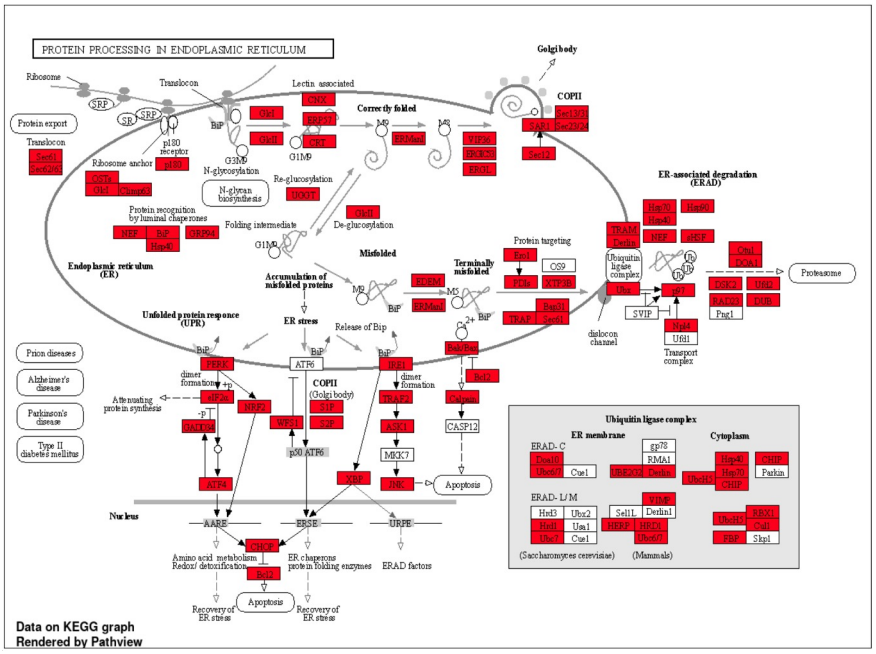

d

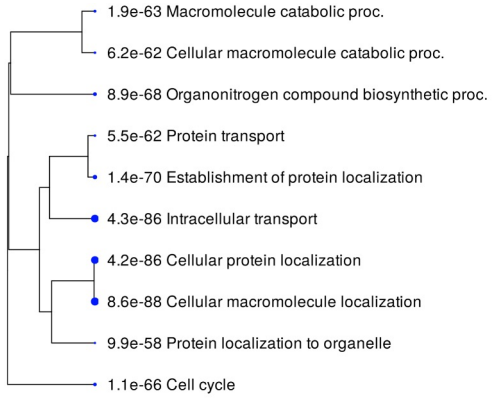

e

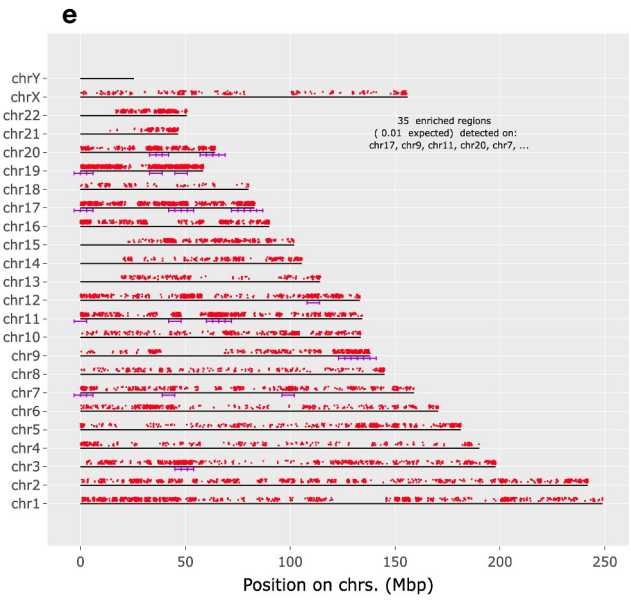

Supplementary Fig. 5 | KEGG pathway analysis of H4K12pr associated genes. **a** Top ten pathways with their number of genes and log2 fold enrichment. FDR is calculated from a nominal *P* value obtained from a hypergeometric test (FDR < 0.05). Fold enrichment is calculated as percentage of H4K12pr differentially-bound genes associated with a pathway divided by the corresponding percentage in input. **b** Protein Processing in ER KEGG pathway enrichment by Pathview. Genes that are overrepresented compared to input are in red. **c** H4K12pr-associated differential binding of key CRC genes and log2 fold changes in their expression levels, as determined by differential RNA-seq of 10 mM treated vs. untreated conditions. n = 3 experimental replicates per condition (FDR < 0.05). **d** Hierarchical clustering tree summary of correlations among significant pathways in H3K18pr-associated annotated genes. Hierarchical clustering of the pathways was performed using ShinyGO. Pathways were clustered together based on shared genes and gene enrichment analysis was performed using two-sided Fisher's exact test, and FDR correction was applied to adjust for multiple comparisons in the pathway analysis and hierarchical clustering. Size of dots indicates statistically significant FDR adjusted (FDR < 0.05) *P* values. **e** Chromosomal position of H3K18pr-associated regions represented by red dots. Purple lines represent statistically significant enrichment compared to input. The genome was scanned with a sliding window (size 6 Mb) further subdivided into 2 equal-sized steps for sliding. Within each window a hypergeometric test was used to test for enrichment over input. FDR-adjusted *P* value cutoff for window was 1E-05. Chromosomes may be partly shown due to scaling to last genes location. Gene chromosomal mapping was performed using ShinyGO.

a

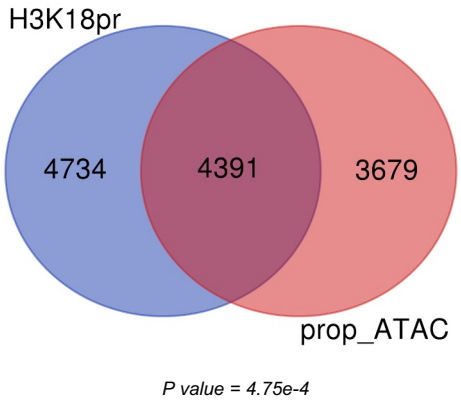

P value = 4.75e-4

b

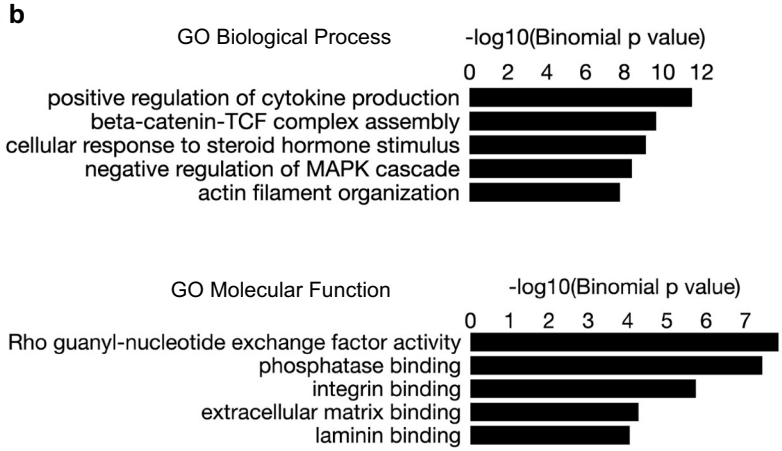

c

H3K18pr ChIP CRC targets — Prop ATAC-seq

symbol	fold	FDR	fold	FDR
CTNNB1	3.00	2.05E-11	0.70	0.0086
TCF20	3.01	9.54E-11	2.24	1.124E-06
LEF1	2.72	9.49E-06	1.32	0.00243
CCND1	3.85	4.08E-21	1.48	5.224E-07
MYC	2.08	9.55E-06	0.81	0.000143
FOS	2.39	1.97E-12	1.46	8.17E-15
JUN	2.67	3.03E-06	1.89	1.76E-16

d

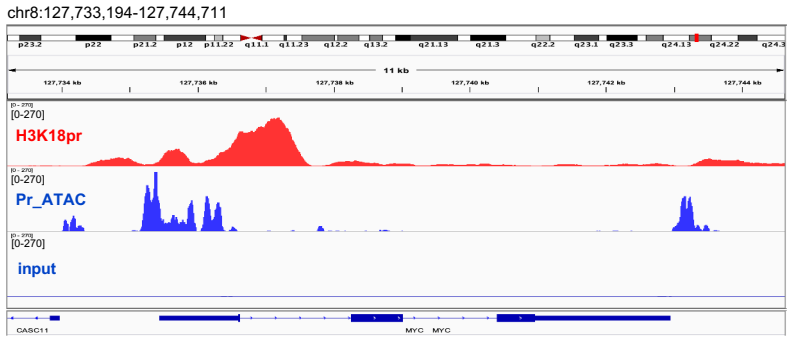

e

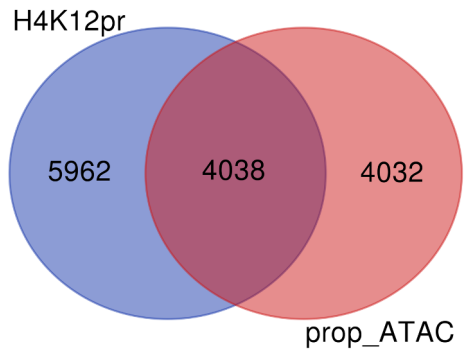

P value = 2.31e-38

f

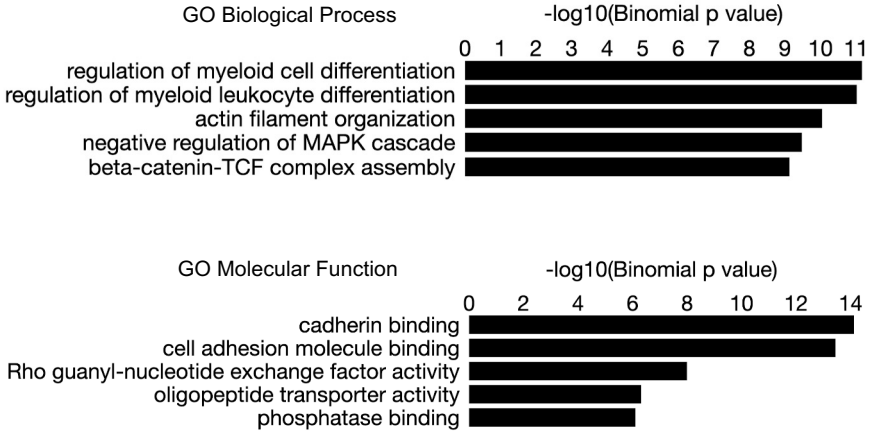

g

H4K12pr ChIP CRC targets — Prop ATAC-seq

symbol	fold	FDR	fold	FDR
CTNNB1	3.17	5.90E-15	0.70	0.0086
TCF20	3.26	0.000136	2.24	1.124E-06
LEF1	2.01	0.0019	1.32	0.00243
CCND1	2.8	5.54E-14	1.48	5.224E-07
MYC	2.4	2.09E-11	0.81	0.000143
FOS	3.05	1.28E-07	1.46	8.17E-15
JUN	3.32	7.54E-18	1.89	1.76E-16

h

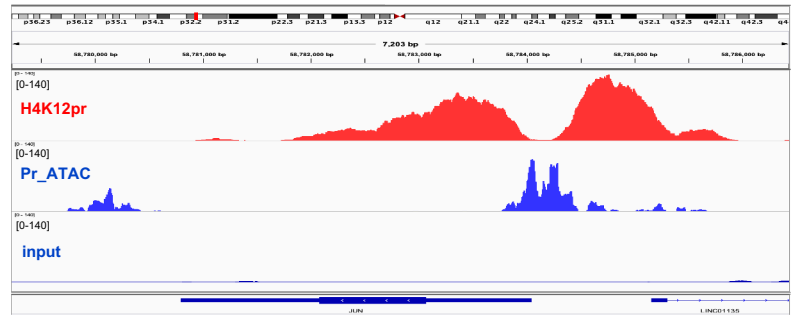

Supplementary Fig. 6 | H3K18/H4K12pr ChIP-seq and propionyl ATAC-seq integration. **a, e** Overlap between TSS-proximal regions (+/- 1 Kb) for H3K18pr and H4K12pr differentially bound genes by ChIP-seq and differentially accessible genes following 10 mM propionate supplementation. Significance of overlap determined by hypergeometric test-generated *P* value. **b, f** GO 'Biological Process' and 'Molecular Function' pathway terms associated with H3K18pr and H4K12pr differentially bound genomic coordinates that are also present in ATAC-seq sorted by binomial *P* value. **c, g** Log2 fold change and FDR-adjusted *P* value in CRC-relevant gene targets associated with H3K18/H4K12pr ChIP-seq and propionyl ATAC-seq. **d, h** Signal tracks for *MYC* and *JUN* regions showing ChIP-seq and ATAC-seq profiles with input as background.

a

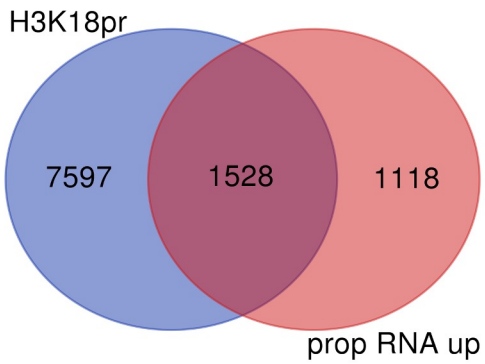

P value = 7.10e-154

b

Enrichment FDR	nGenes	Fold Enrichment	Pathways
2.1E-19	159	2.2	Cell morphogenesis
1.4E-20	214	2	Generation of neurons
9.3E-19	194	2	Neuron differentiation
2.0E-19	207	2	Cell migration
8.4E-21	228	2	Neurogenesis
9.3E-19	210	1.9	Plasma membrane bounded cell projection organization
2.0E-19	224	1.9	Cell motility
2.0E-19	224	1.9	Localization of cell
1.5E-18	213	1.9	Cell projection organization
1.1E-20	247	1.9	Locomotion

c

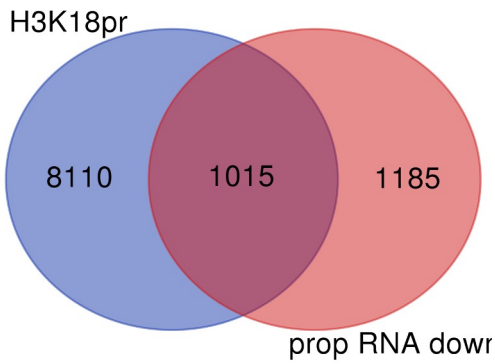

P value = 3.29e-12

d

Enrichment FDR	nGenes	Fold Enrichment	Pathways
4.7E-20	88	3.3	Mitotic cell cycle phase transition
4.4E-34	145	3.2	Mitotic cell cycle proc.
9.0E-35	152	3.2	Chromosome organization
9.4E-36	160	3.1	Mitotic cell cycle
9.9E-26	120	3.1	Reg. of cell cycle proc.
3.9E-26	131	2.9	MRNA metabolic proc.
8.4E-35	183	2.8	Cell cycle proc.
4.6E-27	147	2.8	Reg. of cell cycle
2.5E-38	226	2.6	Cell cycle
1.2E-20	184	2.1	Pos. reg. of macromolecule biosynthetic proc.

e

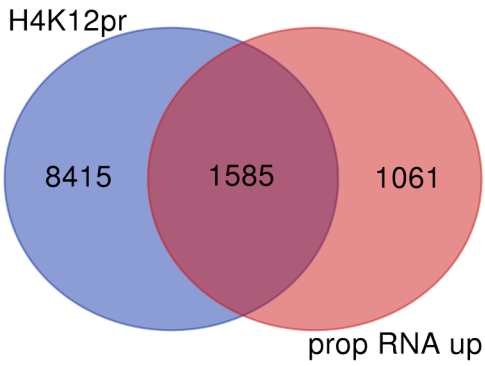

P value = 1.69e-147

f

Enrichment FDR	nGenes	Fold Enrichment	Pathways
5.2E-15	118	2.3	Actin cytoskeleton organization
7.8E-15	120	2.3	Cell morphogenesis involved in differentiation
5.4E-15	127	2.2	Localization within membrane
7.8E-15	127	2.2	Actin filament-based proc.
6.4E-18	161	2.2	Cell morphogenesis
5.4E-15	196	1.9	Cytoskeleton organization
9.7E-15	201	1.8	Generation of neurons
2.0E-15	217	1.8	Neurogenesis
3.0E-14	231	1.7	Locomotion
3.3E-14	230	1.7	Cellular macromolecule localization

g

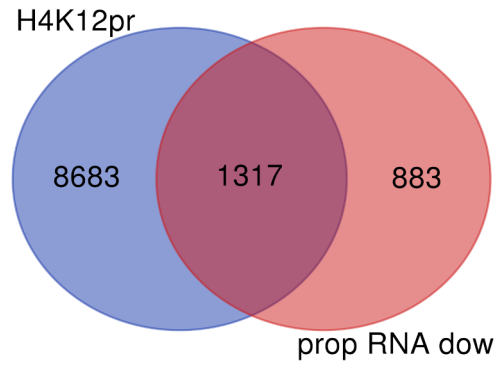

P value = 1.35e-167

h

Enrichment FDR	nGenes	Fold Enrichment	Pathways
2.4E-36	107	4.3	Reg. of mRNA metabolic proc.
4.2E-37	118	4	RNA splicing
1.0E-51	199	3.4	MRNA metabolic proc.
1.5E-42	191	3.1	Chromosome organization
4.2E-37	174	3	Mitotic cell cycle proc.
1.2E-40	195	2.9	Mitotic cell cycle
7.4E-38	186	2.9	RNA processing
7.1E-37	192	2.8	Reg. of cell cycle
2.2E-44	234	2.7	Cell cycle proc.
1.6E-47	286	2.5	Cell cycle

Supplementary Fig. 7 | H3K18/H4K12pr ChIP-seq and propionyl RNA-seq integration. Overlap between TSS-proximal regions (+/- 1 Kb) for H3K18pr and H4K12pr associated genes by ChIP-seq, and upregulation of gene expression in 10 mM NaPr treated group **a**, **e** vs downregulation in the untreated group **c**, **g** by RNA-seq. Significance of overlap determined by hypergeometric test-generated *P* value. GO 'Biological Process' pathway terms associated with overlapping Kpr targets and upregulated genes **b**, **f** and downregulated genes **d**, **h** sorted by log2 fold enrichment.

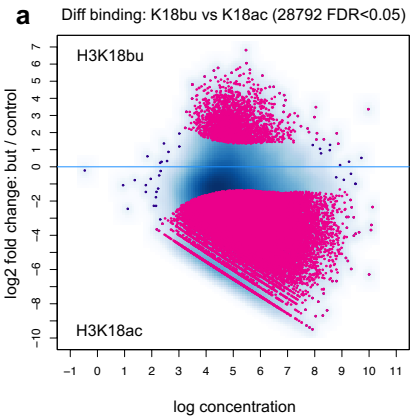

b

H3K18bu ChIP-seq: Top 10 differentially bound regions

Coordinates | shortest distance		Symbol	log2fold	FDR
chr8:	127036104 43269	*PRNCR1*	3.37	2.25E-09
chr16:	52456088 18084	*TOX3*	5.46	9.76E-09
chr18:	70376493 3146	*LINC01910*	6.05	1.19E-08
chr15:	80750026 5094	*ABHD17C*	4.78	1.24E-08
chr15:	80750026 28816	*CEMIP*	4.78	1.24E-08
chr14:	55807471 10784	*LINC00520*	5.67	1.25E-08
chr2:	14628553 3632	*LRATD1*	5.1	1.25E-08
chr6:	163574167 3928	*QKI*	4.94	1.41E-08
chr18:	37484062 81474	*CELF4*	5.17	1.56E-08
chr8:	91345780 62427	*CRAT37*	4.59	1.57E-08

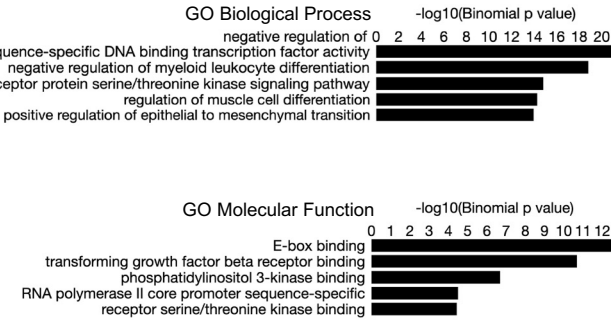

d

Smad3 (**MAD motif**)

P value	fold	% targets	% background
1e-1555	3.07	43.74	22.06

Foxo1 (**Forkhead motif**)

P value	fold	% targets	% background
1e-1665	3.67	35.20	15.01

KLF5 (**Zf motif**)

P value	fold	% targets	% background
1e-1175	4.04	22.30	8.52

KLF14 (**Zf motif**)

P value	fold	% targets	% background
1e-1445	3.94	27.69	10.86

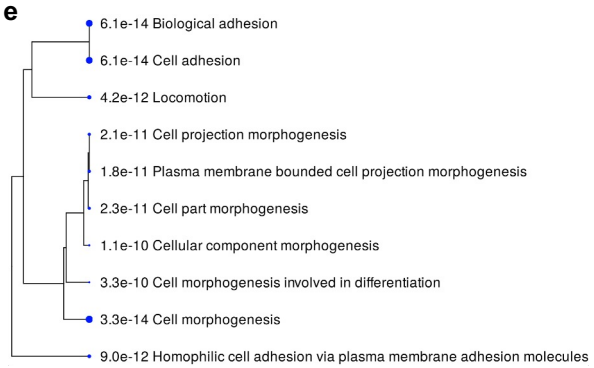

f

chr8:127,036,105-127,036,605

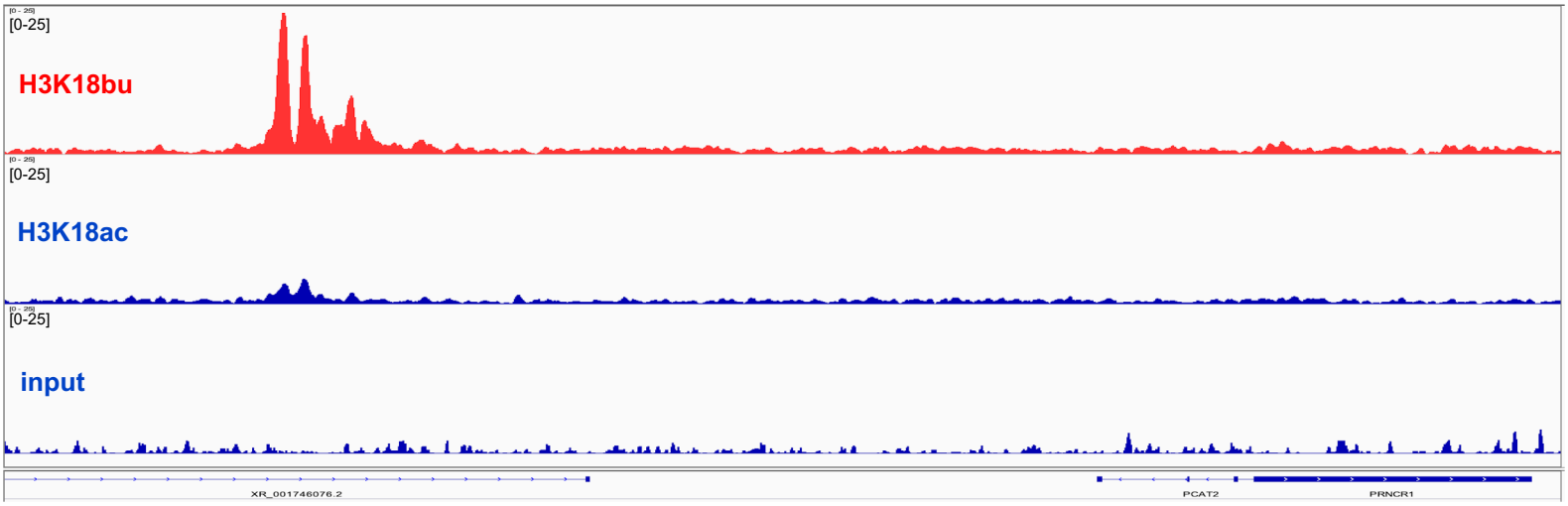

Supplementary Fig. 8 | Genome-wide H3K18bu distribution. **a** H3K18bu vs H3K18ac differential binding following 1 mM butyrate supplementation. Sites identified as significantly differentially bound are shown in red. Differential binding was performed by DiffBind package with DESeq2 using a two-sided tests for both increased and decreased binding affinity between conditions followed by by multiple hypothesis testing and FDR correction. **b** Top ten differentially bound regions associated with H3K18bu sorted by false-discovery rate adjusted *P* value (FDR < 0.05). **c** Top GO 'Biological Process' and 'Molecular Function' terms associated with H3K18bu-bound *cis*-regulatory elements determined by GREAT against a whole genome background using a binomial test over genomic regions, followed by multiple hypothesis testing using FDR corrected *P* values (FDR < 0.05). **d** Differential motif analysis of H3K18bu vs H3K18ac peaks was analyzed by HOMER, using a one-sided hypergeometric test for overrepresentation (enrichment) of motifs in the target sequences compared to the background, followed by multiple hypothesis testing and FDR correction. **e** Hierarchical clustering tree summary of correlations among significant pathways in H3K18pr-associated annotated genes. Hierarchical clustering of the pathways was performed using ShinyGO. Pathways were clustered together based on shared genes and gene enrichment analysis was performed using two-sided Fisher's exact test, and FDR correction was applied to adjust for multiple comparisons in the pathway analysis and hierarchical clustering. Size of dots indicates statistically significant FDR adjusted (FDR < 0.05) *P* values. **f** Signal tracks of 71 Kb-spanning *PRNCR1* region showing H3K18bu vs H3K18ac binding with input as background.

a

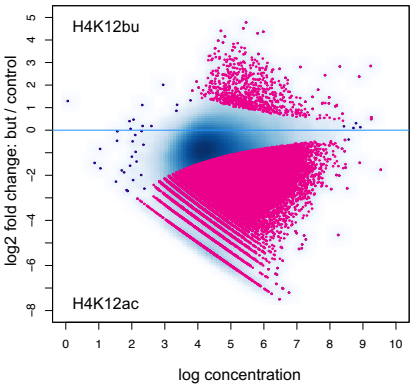

b

H4K12bu ChIP-seq: Top 10 differentially bound regions					
Coordinates | shortest distance			Symbol	log2fold	FDR
chr8:	127036130	43243	*PRNCR1*	2.85	3.14E-77
chr7:	20217130	273	*MACC1*	2.8	6.53E-19
chr1:	198621156	17014	*PTPRC*	2.98	4.36E-13
chr15:	91345559	62648	*CRAT37*	4.52	6.85E-13
chr6:	129491243	24825	*LAMA2*	2.69	1.15E-12
chr8:	126842123	4431	*PCAT1*	2.83	1.57E-12
chr3:	114706917	392417	*ZBTB20*	3.05	1.03E-11
chr7:	138890353	58973	*KIAA1549*	2.71	1.70E-11
chr2:	105583190	144678	*FHL2*	2.58	1.77E-11
chr10:	62933853	13954	*EGR2*	2.68	4.19E-11

c

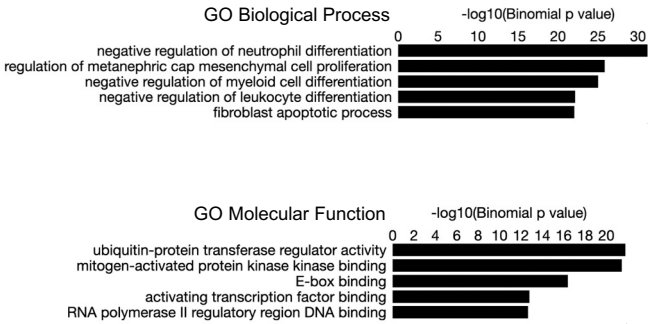

d

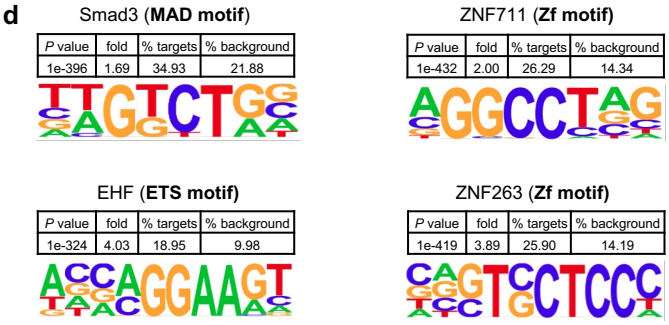

e

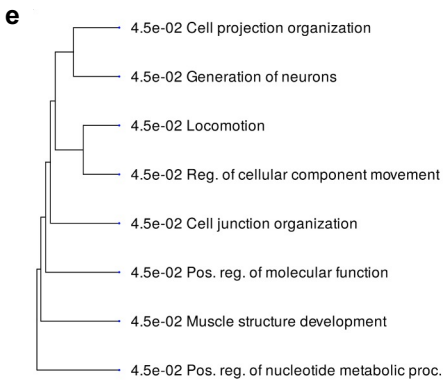

f

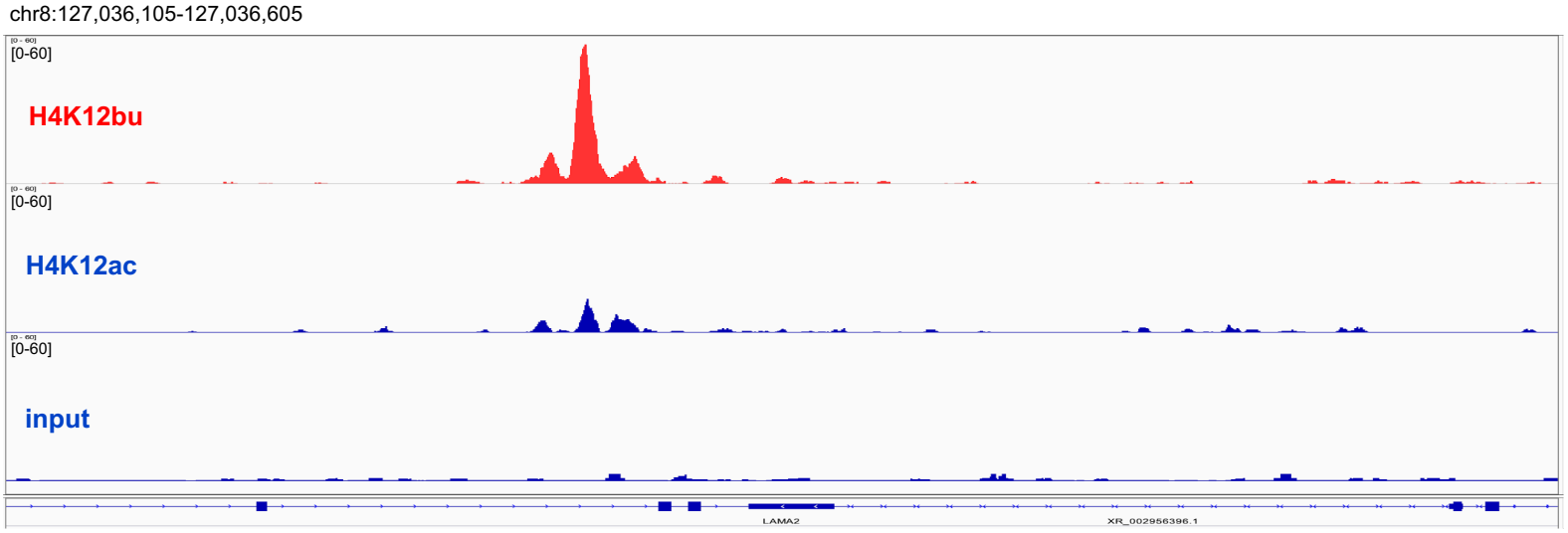

Supplementary Fig. 9 | Genome-wide H4K12bu distribution. **a** H4K12bu vs H4K12ac differential binding following 1 mM butyrate supplementation. Sites identified as significantly differentially bound are shown in red. Differential binding was performed by DiffBind package with DESeq2 using a two-sided tests for both increased and decreased binding affinity between conditions followed by by multiple hypothesis testing and FDR correction. **b** Top ten differentially bound regions associated with H4K12bu sorted by false-discovery rate adjusted *P* value (FDR < 0.05). **c** Top GO 'Biological Process' and 'Molecular Function' terms associated with H3K18bu-bound *cis*-regulatory elements determined by GREAT against a whole genome background using a binomial test over genomic regions, followed by multiple hypothesis testing using FDR corrected *P* values (FDR < 0.05). **d** Differential motif analysis of H4K12bu vs H4K12ac peaks was analyzed by HOMER, using a one-sided hypergeometric test for overrepresentation (enrichment) of motifs in the target sequences compared to the background, followed by multiple hypothesis testing and FDR correction. **e** Hierarchical clustering tree summary of correlations among significant pathways in H4K12bu-associated annotated genes. Hierarchical clustering of the pathways was performed using ShinyGO. Pathways were clustered together based on shared genes and gene enrichment analysis was performed using two-sided Fisher's exact test, and FDR correction was applied to adjust for multiple comparisons in the pathway analysis and hierarchical clustering. Size of dots indicates statistically significant FDR adjusted (FDR < 0.05) *P* values. **f** Signal tracks of 20 Kb-spanning *LAMA* region showing H4K12bu vs H4K12ac binding with input as background.

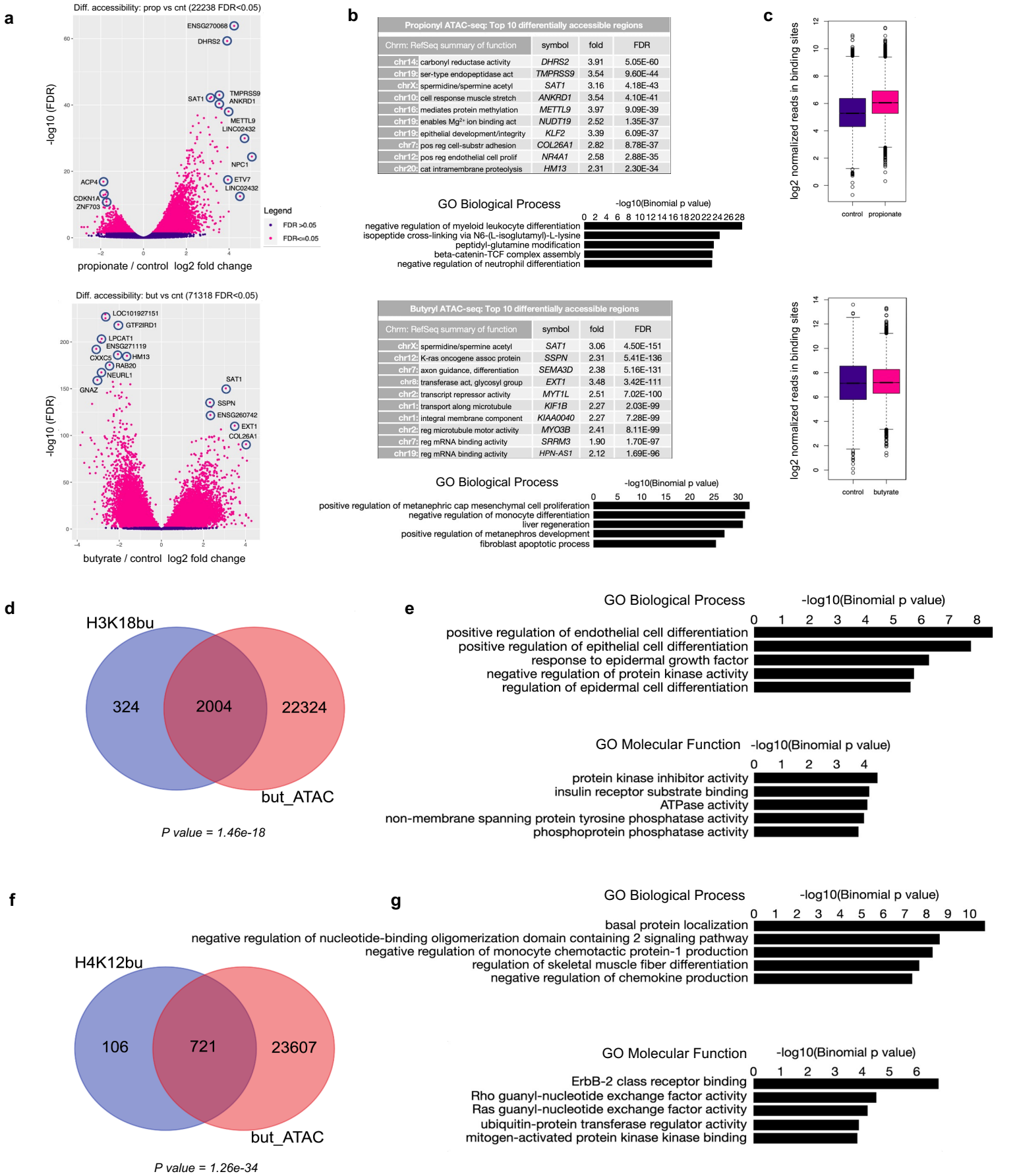

Supplementary Fig. 10 | Propionyl and butyryl ATAC-seq and Kbu ChIP-seq and ATAC-seq integration. **a** Differential accessibility following propionate and butyrate supplementation. Sites identified as significantly differentially accessible are shown in red. n = 3 technical replicates for each condition. Differential accessibility was performed by DiffBind package with DESeq2 using a two-sided tests for both increased and decreased binding affinity between conditions followed by by multiple hypothesis testing and FDR correction. **b** Top ten differentially bound regions associated with propionate and butyrate treatment sorted by false-discovery rate adjusted *P* value (FDR < 0.05) and top GO 'Biological Process' terms determined by GREAT against a whole genome background using a binomial test over genomic regions, followed by multiple hypothesis testing using FDR corrected *P* values (FDR < 0.05). **c** Normalized reads in accessible sites following propionate and butyrate treatment. Box plots display: The minimum, first quartile (Q1, 25th percentile), median, third quartile (Q3, 75th percentile), and maximum. The bottom of the box is Q1 and the top of the box is Q3. The line within the box represents the median (50th percentile) value. The whiskers extend to the most extreme data points within 1.5 times the IQR (interquartile range). **d, f** Overlap between Kbu bound genes and differentially accessible regions following 1 mM butyrate treatment. Significance of overlap determined by hypergeometric test-generated *P* value. **e, g** GO 'Biological Process' and 'Molecular Function' pathway terms associated with Kbu bound genomic coordinates that are also present in ATAC-seq data set sorted by binomial *P* value.